# Exploration of the Hydrogen Sulfide−Germanium Sulfide System

Jacob T. Sutherland, Steven A. Poling, Renaud C. Belin, and Steve W. Martin*

*Department of Materials Science & Engineering, Iowa State University, Ames, Iowa 50011*

*Received October 10, 2003. Revised Manuscript Received December 30, 2003*

In the present work, the $(x)H_2S + (1-x)GeS_2$ system has been systematically investigated to determine the incorporation of hydrogen into the tetrahedral germanium sulfide network. Reactions between gaseous $H_2S$ and glassy-$GeS_2$ have been explored over a range of temperatures and pressures. Reactions for shorter times and lower temperatures (ambient through ~250 °C) produced the protonated thiogermanic acid $H_4Ge_4S_{10}$ with an adamantane-like microstructure. In contrast, longer reaction times produced the unprotonated low-temperature three-dimensional α-$GeS_2$ crystal structure. At higher temperatures (~750 °C), sublimation reactions produced weakly protonated amorphous materials in the form of spherical particles (100 nm to a few μm). Structural characterizations of the obtained amorphous and crystalline materials have been performed using IR and Raman spectroscopies, thermogravimetric analysis, ac impedance spectroscopy, and SEM. Thermal mass loss measurements and quantitative IR of the S−H stretching region ~2500 $cm^{-1}$ were used to determine the amount of hydrogen incorporated into the $GeS_2$ network.

## Introduction

Germanium disulfide ($GeS_2$)-based systems have received attention recently for a number of different reasons. $GeS_2$ is a good glass former and some $GeS_2$-based glasses exhibit both favorable electrical and optical properties. Semiconducting glasses such as the Ge−Ga chalcogenides, for example, $GeS_2-Ga_2S_3$ glasses, are potential materials for microelectronics devices.[1,2] The low phonon energy of glassy-$GeS_2$ (g-$GeS_2$) makes it an attractive choice for 1.3-μm optical fiber amplification.[3,4] Additionally, $GeS_2$ is one of several materials that has attracted the attention of researchers in the area of fast ion-conducting glasses for battery applications[5,6] and proton-conducting membranes.[7,8] Bulk binary glasses such as the $Ag_2S + GeS_2$ or $Li_2S + GeS_2$ systems are solid electrolytes with a high ionic conductivity at room temperature.[9,10]

Interestingly, the simplest system of the modified thiogermanates, $H_2S + GeS_2$, appears to have never been extensively studied.[11,12] Recently, an adamantane-like $H_4Ge_4S_{10}$ phase was prepared and structurally characterized from liquid $H_2S$ reactions with quartz-type $GeO_2$[7,8] and glassy $GeS_2$.[13] Additionally, a double-decker-like $H_2Ge_4S_9$ phase was suggested from prolonged liquid $H_2S$ reactions with quartz-type $GeO_2$.[7] Figure 1 shows an example of the $H_4Ge_4S_{10}$ thio-acid with an adamantane-like $[Ge_4S_{10}]^{4-}$ anion. The $GeO_2$ reactions were effectively hydrated, as $H_2O$ is a product from the $H_2S$ and $GeO_2$ reactants. In prior work, a stoichiometric $H_2Ge_2S_5$ phase was reported to have been produced from a hydrous form of $GeO_2$ in a $H_2S$ saturated solution.[14,15] In each of these reports, the presence of water is suggested in the reaction process.

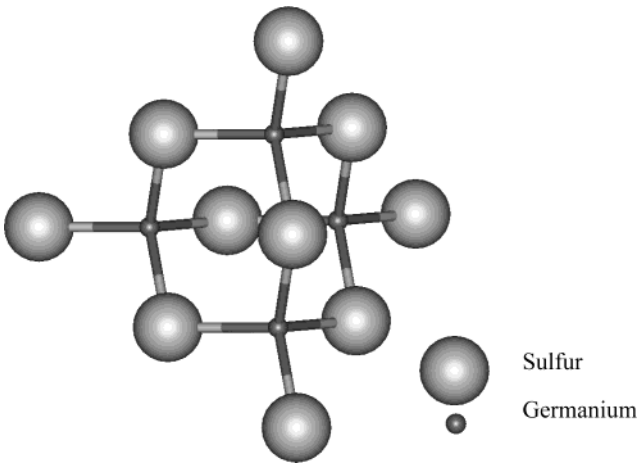


**Figure 1.** Adamantane-like $[Ge_4S_{10}]^{4-}$ anion for the $H_4Ge_4S_{10}$ thiogermanic acid.

* To whom correspondence should be addressed.

(1) Julien, C.; Barnier, S.; Massot, M.; Chbani, N.; Cai, X.; Loireau-Lozac'h, A. M.; Guittard, M. *Mater. Sci. Eng.* **1994**, *B22*, 191.
(2) Fontana, M.; Rosi, B.; Ivanova, Z.; Kirov, N. *Philos. Mag.* **1987**, *B56*, 507.
(3) Simons, D.; Faber, A.; Dewaal, H. *J. Non-Cryst. Solids* **1995**, *185*, 283.
(4) Marchese, D.; Kakarantzas, G. *J. Mod. Opt.* **1996**, *43* (5), 963.
(5) Martin, S. *J. Am. Ceram. Soc.* **1991**, *74*, 1767.
(6) Martin, S. *J. Non-Cryst. Solids* **1986**, *83*, 185.
(7) Poling, S.; Sutherland, J.; Nelson, C.; Martin, S. *J. Phys. Chem. B* **2003**, *107*, 5413.
(8) Poling, S.; Sutherland, J.; Nelson, C.; Martin, S. *Solid State Ionics*, in press.
(9) Souquet, J.; Robinel, E.; Barrau, B.; Ribes, M. *Solid State Ionics* **1981**, *3* (4), 317.
(10) Pradel, A.; Ribes, M. *Mater. Chem. Phys.* **1989**, *23*, 121.
(11) O'Hare, P. *J. Chem. Thermodyn.* **1987**, *19*, 675.
(12) O'Hare, P. *J. Chem. Thermodyn.* **1995**, *27*, 99.
(13) Poling, S.; Sutherland, J.; Nelson, C.; Martin, S. *Inorg. Chem.*, **2003**, *42*(23), 7372.
(14) Willard, H.; Zuehlke, C. *J. Am. Chem. Soc.* **1943**, *65*, 1887.
(15) Pascal, P. *Traité de Chimie Minérale, Tome V.;* Editions Masson et cie: Paris, 1968; p 138.

10.1021/cm034990+ CCC: $27.50 
Published on Web 03/02/2004

Other researchers have prepared thiogermanic acids in the form of potassium salts.[14] The meta-thiogermanic acid ($H_2GeS_3$) has been obtained in the form of the piperazine salt ($H_2GeS_3$:$C_4H_{10}N_2$ or $S_2GeC_4H_{10}N_2$, $H_2S$)[16] and the pyro-thiogermanic acid ($H_6Ge_2S_7$) in the form of the sodium and potassium salts.[17]

Recent work at lower temperatures on the $H_2S$ + $GeS_2$ system has yielded an efficient method to quickly produce pure α-$GeS_2$,[18] which is the low temperature, three-dimensional crystalline phase of $GeS_2$. In the present work, the $xH_2S + (1-x)GeS_2$ system has been systematically investigated with respect to reaction temperature. A new synthesis route involving gaseous reactions between $GeS_2$ and $H_2S$ has been developed. Both high (∼750 °C) and more moderate temperatures (25−250 °C) have been explored. SEM micrographs of the materials produced from high-temperature reactions are shown for comparison. A temperature-dependent reaction route is proposed based on Raman and IR spectroscopy. A calibration plot of the concentration dependence of the IR absorption in the S−H stretch region (∼2500 $cm^{-1}$) is presented. Quantitative IR is then performed, via a calibration plot, for select samples and compared to mass loss and Raman results. Conductivity data is also measured for comparison.

## Experimental Section

**Preparation and Characterization of the Materials.** Glassy-$GeS_2$ (g-$GeS_2$) was prepared from stoichiometric amounts of germanium (Cerac, 99.999%, 100 mesh) and sulfur (Alfa Aesar, 99.999%, 325 mesh) sealed under vacuum in a silica tube heated at 3 °C/min to 900 °C in a rotating furnace for 8 h. After air quenching, the glassy product was ground to a fine powder in a spex-mill. Raman and mid-IR spectroscopies were used to verify its purity with regard to crystallinity and hydrogen and oxide contaminates. To avoid the possibility of air and moisture contamination, a helium glovebox (<5 ppm $O_2$ and $H_2O$) was used for all handling of starting and final materials.

All IR spectra of the materials were produced using a 3 wt % sample to KBr in pressed pellets. The IR spectra were measured with a Bruker IFS 66v/s IR spectrometer using 4-$cm^{-1}$ resolution. Raman spectra were taken with a Bruker RFS-100/S FT-Raman spectrometer using a Nd:YAG 1064-nm laser line, liquid nitrogen Ge detector in a 180° backscattering geometry and 4-$cm^{-1}$ resolution.

Investigation of the weight loss as a function of temperature for the reaction products was preformed using a Perkin-Elmer Thermogravimetric Analyzer TGA 7 (TGA). A 20 mL/min flow of $N_2$ was employed to minimize sample oxidation. About 25 mg of each sample was placed into a small aluminum pan and heated at a rate of 10 °C/min from 50 to 500 °C.

Select samples were also investigated with SEM and impedance spectroscopy. The SEM micrographs were produced with an Hitachi S-2460N Environmental SEM with a Gresham light element X-ray detector using Isis microanalysis by Oxford. The impedance spectroscopy was performed with a Gamry PC4/750 potentiostat using 500-mV amplitude voltage in the frequency range of $10^{-1}-10^5$ Hz on pressed powder samples. About 50 mg of each sample was pressed inside a 0.25-in i.d. alumina tube using ∼82 ksi; this resulted in pellet thicknesses of ∼0.6 mm. Stainless steel electrodes were pressed to the sample using a metal frame, which was electrically insulated with alumina. The constant electrode pressure on the pressed samples helped to minimize any interfacial separation of the powder and aided in maintaining a constant pellet density. An atmosphere of helium was employed inside the silica conductivity cell, which was heated using a laboratory-constructed furnace. Each sample was allowed to thermally stabilize for 30 min at each temperature before data collection commenced. Cole−Cole complex impedance plane plots were used to acquire the bulk resistivity of the sample represented by the intersection of the depressed semicircles. Cell constants were determined from the thickness of the pressed sample and the area of the electrodes.

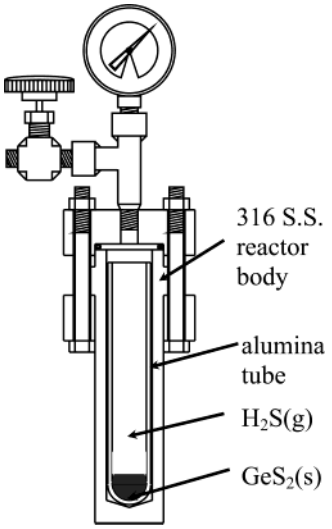


**Figure 2.** A schematic drawing of the type 316 stainless steel reactor that was used in the moderate temperature ($T$ < 250 °C) experiments.

**Moderate-Temperature Reactions.** Figure 2 presents a schematic drawing of the stainless steel-type 316 reactor that was used in the high-pressure (∼290 psig) moderate-temperature (<250 °C) experiments. For each reaction, 200 ± 1 mg of g-$GeS_2$ was placed in a dried alumina tube (closed one end), which was then placed into the reactor. A Viton O-ring was used to seal the bottom tube portion of the reactor to the top assembly with a Swagelok valve. The reactor was then evacuated to ∼75 mTorr. The bottom portion of the reactor was cooled with liquid nitrogen and back-filled with ∼2.2 g of $H_2S$ (∼270 psig at ambient temperature). The reactor was then allowed to warm back to ambient temperature and placed in a water bath held at 30.0 ± 0.5 °C. The $H_2S$ gas was bled out of the reactor until a pre-reaction pressure, depending on the ultimate reaction temperature, was achieved. The specific pre-reaction pressure was calculated using the equation of state of $H_2S$,[19] once the reactor reached its intended reaction temperature (50−225 °C), the pressure would be 290 psig.

The reactor subsequently was placed in a second liquid nitrogen bath inside a $N_2$ glovebox. The reactor top assembly with Swagelok valve was replaced with a steel blank and sealed with a Teflon O-ring after the reactor had reached liquid nitrogen temperatures with the $H_2S$ inside frozen solid.

Finally, the assembled reactor was placed into a furnace preheated to a specific reaction temperature. After the designated reaction time of ∼16 h the reactor was removed and allowed to cool to ambient laboratory temperature. The reactor was again placed into a $N_2$ glovebox and cooled to liquid nitrogen temperatures. The steel blank top was then replaced with the top assembly with Swagelok valve and sealed with a Viton O-ring. After removal from the glovebox, the reactor again was allowed to warm to ambient laboratory temperature. Finally, the $H_2S$ was removed from the reactor by passing it through a solution of $NH_4OH$.

**High-Temperature Reactions.** To facilitate gaseous reactions between $H_2S$ and $GeS_2$, a pressurized system was

(16) Debucquet, L.; Vella, L. *Bull. Soc. Chim.*. **1932**, *51*, 1565.
(17) Schwarz. *Gieze. Ber.* **1930**, *63*, 779.
(18) Sutherland, J.; Poling, S.; Nelson, C.; Martin, S. *Mater. Sci. Lett.* **2003**, *22*(21), 1467.
(19) Rau, H.; Mathia, W. *Ber. Bunsen-Ges. Phys. Chem.* **1982**, *86*, 108.

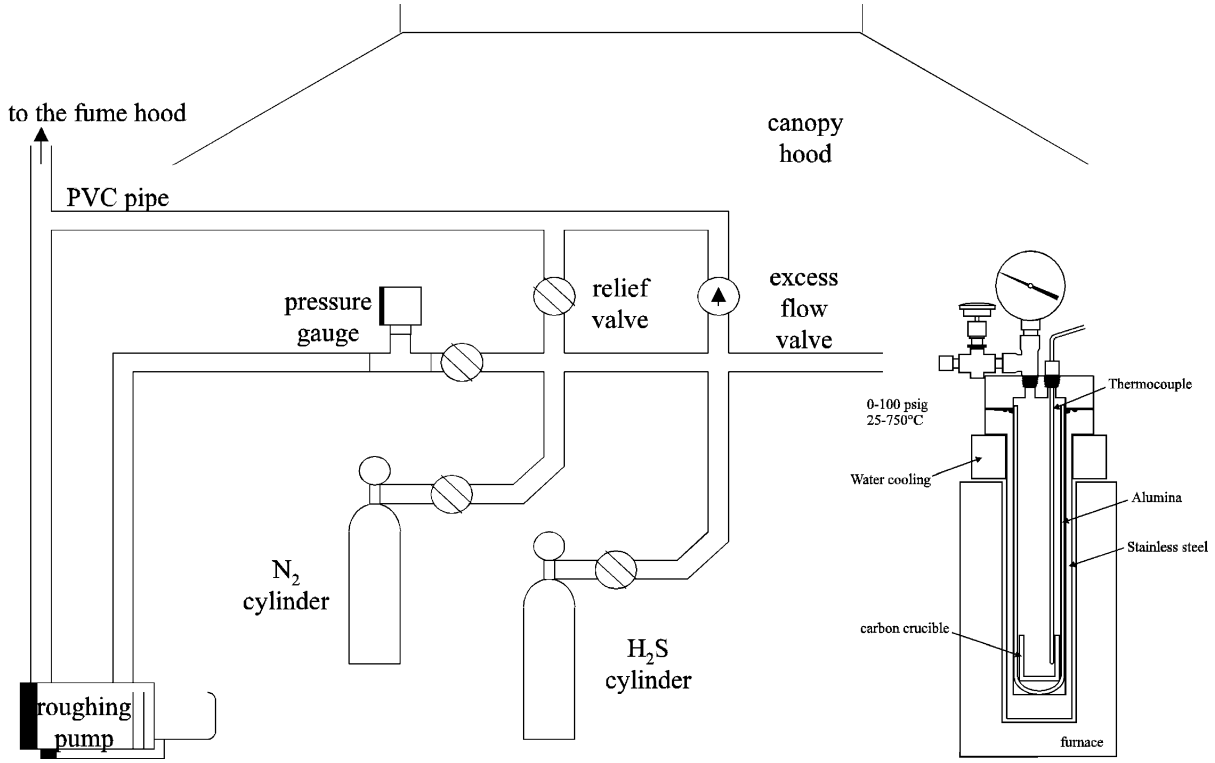


**Figure 3.** A schematic drawing of the system used to pressurize both the high- and moderate-temperature reactors. Also depicted is a schematic drawing of the water-cooled stainless steel-type 310 reactor that was used in the high-temperature $T = \sim 750$ °C experiments.

constructed as shown in Figure 3. This system allows the reaction between $H_2S$ and $GeS_2$ up to ~100 psig and at temperatures up to ~750 °C. It is composed of a type 310 stainless steel reaction vessel with an alumina tube (closed one end) placed inside. The reactor is sealed at the top with a Viton O-ring that is held below its working temperature of ~232 °C using a water-cooled brass collar. The bottom portion of the reactor is placed in a crucible furnace; the reactor is connected to the system and evacuated (~75 mTorr) and back-filled with $H_2S$ gas (Matheson Tri-Gas Company with 99.9 mol % purity and ~0.05 mol % $H_2O$ as contaminate) as shown in Figure 3.

High-temperature protonation experiments were conducted by placing ~3 g of $GeS_2$ in a vitreous carbon crucible inside the reactor. The initial pressure of $H_2S$ at room temperature was ~30 psig. The reactor was heated to ~750 °C at a rate of 5 °C/min where the maximum pressure was ~100 psig. It was found that, after a short time, the $GeS_2$ sublimated and a very thin deposit of brown powder was collected in the water-cooled upper portion of the reactor. While different phases were expected at different temperatures, it was found that all high-temperature reactions yielded the same product of sulfur deficient g-$GeS_2$. It was also noticed that if the initial pressure was higher than ~30 psig, defect amounts of hydrogen were incorporated into the material at elevated temperatures (~750 °C).

## Results and Discussion

**Moderate-Temperature Reaction Products.** The Raman spectra of select glass-ceramic samples produced below 250 °C are shown in Figure 4; it is clear that samples A and B are both mostly glassy whereas samples C and D are primarily the adamantane-like phase. Sample E is predominantly α-$GeS_2$, or the lower temperature three-dimensional phase of $GeS_2$, as indicated by the weaker intensity peaks at 372 and 381 $cm^{-1}$. [20] Table 1 details the predominate component of each of the five selected samples. The corresponding mass loss recorded by TGA measurements for each

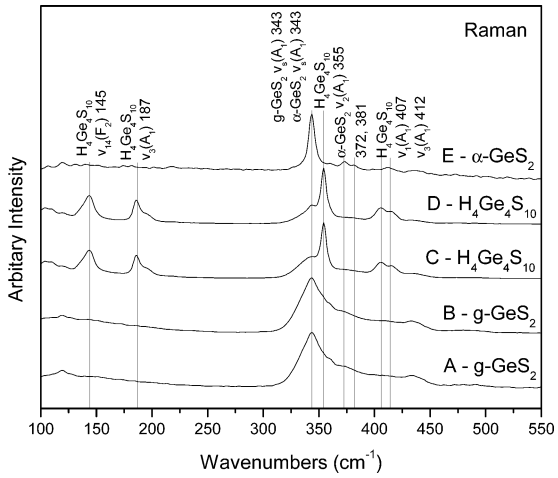


**Figure 4.** Raman spectra of selected TGA samples in Figure 9 prior to thermal measurement. Samples A and B show effectively unreacted products, consistent with g-$GeS_2$. Samples C and D are consistent with the of $H_4Ge_4S_{10}$ phase. Sample E is consistent with α-$GeS_2$. This reinforces the suggested reaction route shown in eq 1.

**Table 1. Predominate Component of Each of the Five Selected Samples (A−E) Is Shown**

| selected samples | primary component |
|---|---|
| A | g-$GeS_2$ |
| B | g-$GeS_2$ |
| C | $H_4Ge_4S_{10}$ |
| D | $H_4Ge_4S_{10}$ |
| E | α-$GeS_2$ |

sample support the phases identified by their Raman spectra. From the TGA thermograms shown in Figure

(20) Kawamoto, Y.; Kawahima, C. *Mater. Res. Bull.* **1982**, *17*, 1511.

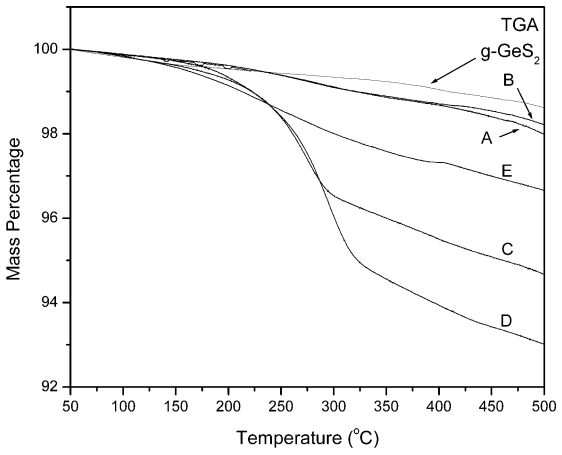


**Figure 5.** TGA spectra of selected glass−ceramic protonated materials produced from moderate-temperature reactions of $H_2S$ + $GeS_2$. Glassy-$GeS_2$ is shown for comparison. Samples A and B show effectively unreacted products; they are consistent with the g-$GeS_2$. Samples C and D are consistent with the $H_4Ge_4S_{10}$ phase. This reinforces the suggested reaction route shown in eq 1.

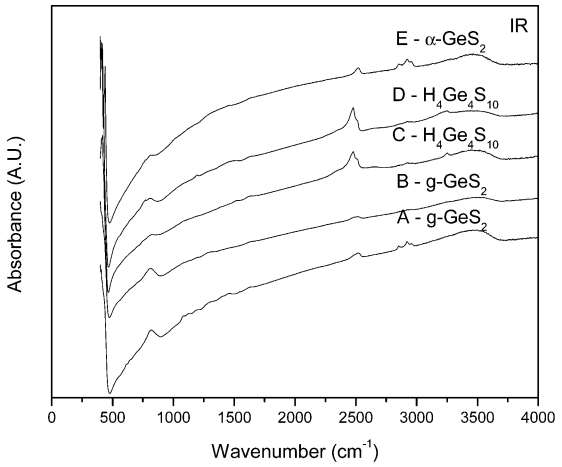


**Figure 6.** IR spectra of selected TGA samples in Figure 9 prior to thermal measurement. Samples A and B show effectively unreacted products and are consistent with g-$GeS_2$. Samples C and D are consistent with the $H_4Ge_4S_{10}$ phase. Sample E is consistent with α-$GeS_2$. This reinforces the suggested reaction route shown in eq 1.

5, samples C and D show an increased mass loss corresponding to the decomposition of the adamantane-like structure above 250 °C.[7]

Infrared spectra are presented in Figure 6 for the corresponding moderate-temperature reaction products of gaseous $H_2S$ and solid $GeS_2$. The IR absorption data are rescaled based on sample concentration and sample thickness to allow a more quantitative comparison between samples. The specific concentration of each sample was determined by density and thickness measurements of the pressed KBr pellet. All of the reactions were performed for ∼16 h at temperatures below 250 °C. The S−H stretch mode at ∼2520 $cm^{-1}$ is the key feature in this figure. It is clear that the protonated phase is an intermediate product for the terminal α-$GeS_2$ phase. In addition to the S−H stretch, several other bands are present in the IR spectra representing contaminates introduced from the starting g-$GeS_2$ precursor. Contamination is noted from the broad bands located around 877 $cm^{-1}$ assigned to asymmetric (Ge−O−Ge) stretching and the broad bands located around 553 $cm^{-1}$ assigned to symmetric (Ge−O−Ge) stretching.[21] $H_2O$ contamination is observed from the O−H stretch mode centered around 3400 $cm^{-1}$. Additionally, a C−H stretching mode at ∼2900 $cm^{-1}$ is present in the spectra representing trace impurities.

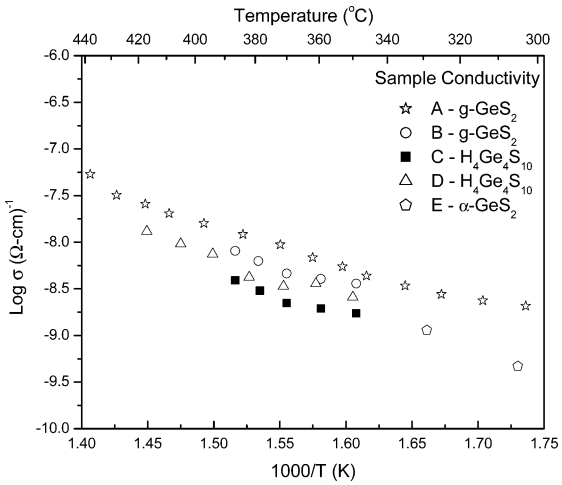


**Figure 7.** Arrhenius plot of dc conductivities of samples (A−E) using pressed powder pellets.

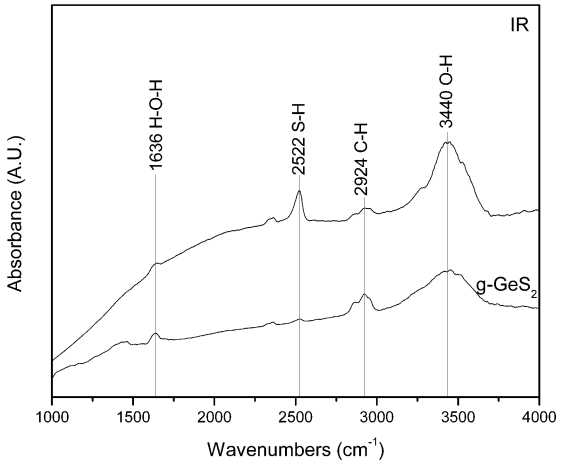


**Figure 8.** IR spectra of weakly protonated amorphous material produced from high-temperature reaction of $H_2S$ with $GeS_2$. Glassy-$GeS_2$ is shown for comparison. The weak bands at 1636 and 3440 $cm^{-1}$ represent $H_2O$ contamination and the weak band at 2924 $cm^{-1}$ is from C−H contamination common in the reactant material.

Arrhenius plots of the dc conductivity for select samples are shown in Figure 7. The conductivities for the mixed phase samples (A−E) are low and of the same magnitude as those previously reported for pure adamantane-like-$H_4Ge_4S_{10}$.[8] Thermal cycling of the samples was not performed due to a high-temperature phase transition attributed to $\beta$-$GeS_2$. The glass transition is indicated by slight discontinuities in the activation energies near ∼360 °C. The conducting species and mechanisms are not clear due to the low conductivities and similar behavior between samples.

**High-Temperature Reaction Products.** The IR spectra of Figure 8 shows a comparison between the starting glassy $GeS_2$ and the resulting weakly protonated product from high-temperature reactions. The

(21) Mernagh, T.; Lin, L. *Phys. Chem. Miner.* **1997**, *24*, 7.

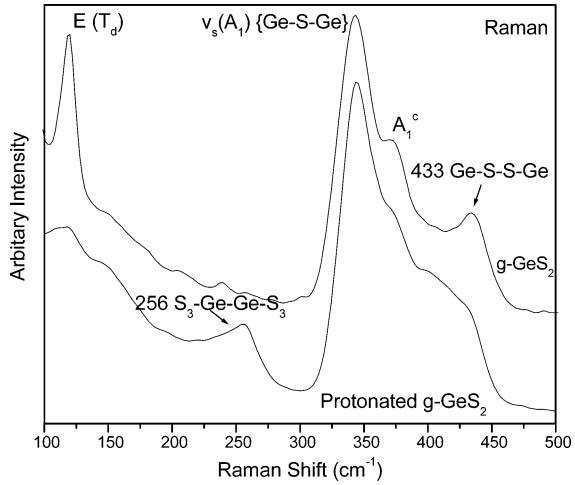


**Figure 9.** Raman spectra of weakly protonated amorphous material from high-temperature reaction of $H_2S$ with $GeS_2$. Glassy-$GeS_2$ is shown for comparison.

weak bands at 1636 and 3440 $cm^{-1}$ represent $H_2O$ contamination and the weak band at 2924 $cm^{-1}$ is from C−H contamination common in the reactant material. The S−H vibration mode around 2500 $cm^{-1}$ is observable only in the reaction products, indicating slight protonation of the material. However, it is not clear when the protonation took place, either during sublimation, ∼750 °C, or after sublimation in the cold zone of the reactor, T <200 °C. The Raman spectra of Figure 9 show that the structure of the protonated g-$GeS_2$-based material is very close to that of the starting g-$GeS_2$. However, there are two main differences. The presence of a new band at ∼250 $cm^{-1}$ can be attributed to ethanelike $S_3Ge-GeS_3$ groups.[22] It is suggested that the synthesis of these groups resulted from reduction of $GeS_2$ via sulfurization of the reactor body at elevated temperatures producing FeS and $FeS_2$. The intensity of this band is small compared to the $GeS_2$ bands and, therefore, the material is mainly composed of $GeS_2$. The second difference is the presence of a new band at 415 $cm^{-1}$ that can be attributed to $Ge-S^-$ bond stretching vibration in dithiogermanate tetrahedra ($GeS_{2.5}^{\ -}$) of $C_{3v}$ symmetry.[7] The rupture of Ge−S−Ge bridges and the formation of thiol groups (S−H) as the network is depolymerized could explain these bands. Other researchers have reported similar features in the silver thiogermanates system.[23]

Figures 10 and 11 show SEM micrographs of the resulting powder that is composed of spherical particles with sizes ranging from ∼100 nm to a few $\mu$m. The particles are found to be very homogeneous with an average composition of 44 and 56 wt % for sulfur and germanium, respectively. This composition corresponds to the formula $GeS_{1.78}$. This result is in accordance with the presence of bands corresponding to $S_3Ge-GeS_3$ contaminates in the Raman spectra.

**Temperature-Dependent Reaction Route.** Structural and mass changes as a function of temperature were investigated using Raman scattering, IR absorption, and TGA mass loss experiments. From these

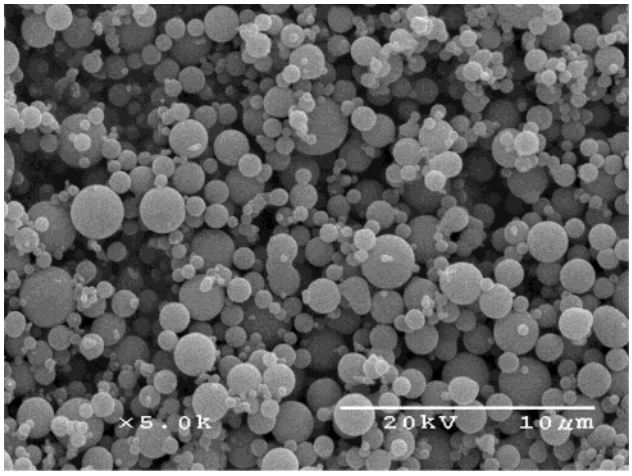


**Figure 10.** SEM micrograph (5000×) of the amorphous protonated material from high-temperature reaction of $H_2S$ with $GeS_2$.

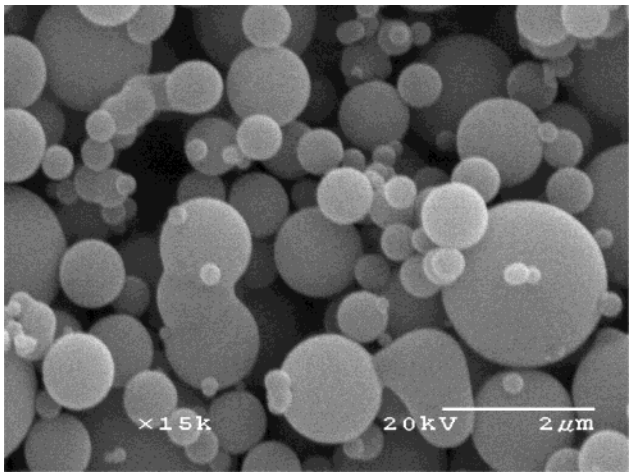


**Figure 11.** SEM micrograph (15000×) of the amorphous protonated material from high-temperature reaction of $H_2S$ with $GeS_2$.

results, the following temperature-dependent reaction route is proposed for the $H_2S-GeS_2$ system:

$$\text{g-}GeS_2 + H_2S(\text{hyd.}) \rightarrow \text{adamantane-}H_4Ge_4S_{10} \rightarrow \alpha\text{-}GeS_2 + H_2S(\text{hyd.}) \quad T < \sim 250\ ^\circ\text{C} \quad (1)$$

The post-script "hyd." has been added to $H_2S$ in the above reaction route to suggest the role of water in the formation of the thiogermanic acid and α-$GeS_2$ phases. Equation 1 states that for temperatures below 250 °C, the protonated thiogermanic phase is initially produced, followed by α-$GeS_2$. A detailed discussion of this reaction has already been reported.[18] In the high-temperature (∼750 °C) sublimation reactions, the resulting product is similar to the starting precursor with only defect quantities of hydrogen.

**Determination of the S−H Concentration.** The IR absorption coefficient of the S−H stretch region in $GeS_2$-based compounds was investigated as a function of the analyte concentration. A calibration plot has been prepared by plotting the absorbance of a series of samples against their analytical concentration.

In this study, various amounts of thiogermanic acid $H_4Ge_4S_{10}$ were mechanically mixed with glassy-$GeS_2$. Mixtures varied from 100 to 0 mol % $H_4Ge_4S_{10}$ with the

(22) Wiley: J.; Buckel, W.; Schmidt, R. *Phys. Rev. B* **1976**, *13* (6), 2489.
(23) Kamitsos, E.; Kapoutsis, J.; Kryssikos, G.; Pradel, A.; Ribes, M. *J. Solid State Chem.* **1994**, *112* (2), 225.

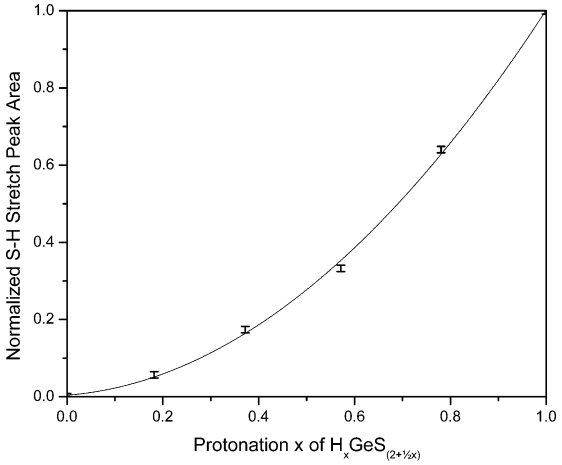


**Figure 12.** Area of the S−H stretch region in the IR absorption spectra of protonated samples as a function of hydrogen concentration (protonation). In this study various amounts of $H_4Ge_4S_{10}$ were mechanically mixed with glassy-$GeS_2$. Collected spectra have been scaled to normalize for mass and thickness variations. On the basis of these results, it is suggested that over a large range in hydrogen concentration the absorption coefficient of the S−H stretch cannot be fit accurately with zero-order polynomial. The fraction of the analyte in the absorbing form is then nonlinear with analyte concentration for S−H in these Ge-based materials.

balance as g-$GeS_2$. The thoroughly mixed samples were then diluted to 3 wt % with KBr. The spectra have been scaled to normalize for mass and thickness variations in the KBr pellets. The area under the S−H stretch was found using a baseline subtraction and then integrating the region. The corresponding areas are shown in Figure 12 as a function of S−H concentration in the samples.

From the Beer−Lambert's Law,

$$A(\lambda,c) = \epsilon(\lambda)\cdot t\cdot c \qquad (2)$$

where $A$ is the measured absorption coefficient (unitless), $\epsilon$ is the wavelength-dependent molar absorptivity coefficient (L/(mol·cm)), $t$ is the thickness of the measured sample (cm), and $c$ is the concentration (mol/L)of the absorbing form of the analyte in the interaction volume. For all of these measurements, the same setup for the IR spectrometer was used, that is, the beam area and intensity was constant between samples. As shown in Figure 12, the absorption fraction of S−H in the absorbing form is nonlinear with actual S−H concentration for these $GeS_2$-based materials.

With use of eq 2 and the absorptivity coefficient determined from the calibration plot shown in Figure 12, the various levels of protonation that were achieved for the moderate-temperature samples (A−E) can be calculated. The same method as outlined in the previous section was used to find the area of the S−H stretch for each glass−ceramic sample. The data are plotted against the reaction temperatures for the samples in Figure 13. Thiogermanic acid $H_4Ge_4S_{10}$ was used to normalize the data as it has a ratio of H to Ge atoms of 1 ($x = 1$); the protonation of the select samples are then shown relative to $H_4Ge_4S_{10}$ ($x < 1$). In Figure 13 a clear trend is indicated; for a reaction time of ∼16 h, protonation is more noticeable at lower temperatures (50 °C). This is consistent with the reaction process as stated in eq 1; that is, at lower temperatures the reaction proceeds slower and the intermediate protonated phase denominates, whereas at higher temperatures the reaction proceeds faster and the terminal α-$GeS_2$ phase is observed. The highest protonation achieved for a glass−ceramic sample was 62% relative to pure $H_4Ge_4S_{10}$.

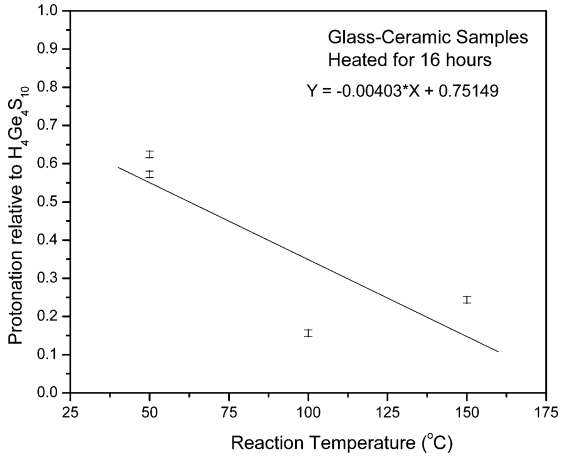


**Figure 13.** Protonation vs reaction temperature of the high-pressure/moderate-temperature materials produced. The protonation ratio of 1:1 is normalized to the thiogermanic acid $H_4Ge_4S_{10}$. The highest protonation achieved for a glass−ceramic sample was 62% relative to $H_4Ge_4S_{10}$.

## Summary and Conclusions

In the present work, the $(x)H_2S + (1-x)GeS_2$ system has been systematically investigated to determine the reaction products of $H_2S$ with $GeS_2$. It is suggested that the terminal stoichiometry that results from protonation of $GeS_2$ with $H_2S$ is consistent with that of the $H_4Ge_4S_{10}$ phase. Two studies were preformed, one at high temperatures (∼750 °C) with moderate pressures (∼100 psig) and the other at moderate temperatures (ambient through ∼250 °C) with higher pressures (290 psig). Structural characterizations of the obtained glass−ceramic materials were carried out using IR and Raman spectroscopies, thermogravimetric analysis, ac impedance spectroscopy, and SEM. Shorter times and lower temperature reactions produce the protonated thiogermanic acid $H_4Ge_4S_{10}$ with an adamantane-like microstructure. Longer times produce an unprotonated low-temperature three-dimensional α-$GeS_2$ crystal structure. Higher reaction temperatures result in weakly protonated glassy materials; the micrograph images show these materials are composed of very small spherical particles (100 nm to a few $\mu$m). Structural incorporation of hydrogen is confirmed by the S−H band in the IR spectrum around 2500 $cm^{-1}$. Quantifiable percentages of protonation (S−H:Ge) are shown as a function of reaction temperature. The highest protonation achieved for the glass−ceramic samples was ∼62% that of $H_4Ge_4S_{10}$.

**Acknowledgment.** Financial support of this work has been provided by the Department of Energy (DE-FC36-00GO10531). Carly R. Nelson is thanked for her assistance with many aspects of the research.

CM034990+